Bulletin of Mathematical Biology Vol. 55, No 4, pp 829–845, 1993
Printed in Great Britain

0092–8240/93$6.00 + 0 00
Pergamon Press Ltd
Society for Mathematical Biology

PATTERN SWITCHING IN HUMAN MULTILIMB COORDINATION DYNAMICS

■ JOHN J. JEKA*, J. A. S. KELSO and TIM KIEMEL†‡
Program in Complex Systems and Brain Sciences,
Center for Complex Systems,
Florida Atlantic University,
Boca Raton, FL 33431, U.S.A.

(*E.mail:jekaebinah.cc.brandeis.edu and kelso@walt.ccs.fav.edu*)

†Mathematical Research Branch, NIDDK,
National Institutes of Health,
Bethesda, MD 20892, U.S.A.

(*E.mail:kiemel@helix.nih.gov*)

A relative phase model of four coupled oscillators is used to interpret experiments on the coordination between rhythmically moving human limbs. The pairwise coupling functions in the model are motivated by experiments on two-limb coordination. Stable patterns of coordination between the limbs are represented by fixed points in relative phase coordinates. Four invariant circles exist in the model, each containing two patterns of coordination seen experimentally. The direction of switches between two four-limb patterns on the same circle can be understood in terms of two-limb coordination. Transitions between patterns in the human four-limb system are theoretically interpreted as bifurcations in a nonlinear dynamical system.

1. Introduction. In the study of biological motor control a primary question is how spatiotemporal patterns (e.g. locomotory patterns) form in systems composed of a large number of components. Theoretically the question is whether their behavior can be described by a few well-chosen state variables, no matter the number of components involved. For example, the behavioral patterns found between two rhythmically moving fingers have been characterized by a single state variable, the relative phase between the fingers (Kelso, 1984). This low-dimensional description was motivated by the assumption that the movement of each finger reflects the output of a distinct oscillator (Haken *et al.*, 1985). From this viewpoint, the coordination between fingers arises from the interactions between two coupled oscillators. Under general assumptions, when oscillators are weakly coupled,

* Present address: Ashton Graybiel Spatial Orientation Laboratory, Brandeis University, Waltham, MA 02254, U.S.A.

‡ Author to whom correspondence should be addressed.

their dynamics are well approximated by a function of their relative phases (Cohen *et al.*, 1982; Ermentrout and Kopell, 1984). Such a relative phase description is also valid in certain cases of strongly coupled oscillators (Ermentrout and Kopell, 1991).

Applying the same approach as above, Schöner *et al.* (1990) proposed a model of quadruped locomotion, using three relative phases as state variables. Assuming left–right and front–hind symmetry they analysed the stability of common *coordination patterns*, i.e. equilibrium points of the dynamics. In this paper we modify the model of Schöner *et al.* and use it to interpret experiments on the coordination between human limbs. We consider changes in the system as a parameter is varied and focus on *pattern switching*: bifurcations in which an equilibrium disappears or becomes unstable and the system moves to another equilibrium point.

2. Summary of Experimental Results.

2.1. *General design of experiments.* In the human multilimb experiments we summarize here (see Kelso and Jeka, 1992, for additional information) a person is seated in a specially designed chair which allows her to rhythmically move her forearms, bending at the elbows, and her lower legs, bending at the knees. All movements are made in planes parallel to the median plane of the body. The position of each limb is characterized by its absolute phase modulo 2π. The absolute phase $0 = 2\pi$ is assigned to the upward peak of a limb's movement and is defined to increase at a constant rate in between upward peaks. The downward peak of a limb's movement occurs at an absolute phase of approximately π. The relative phase ϕ between two limbs is defined as the difference in their absolute phases. If two limbs are in-phase ($\phi \approx 0$), both are moving up and down together, while if two limbs are anti-phase ($\phi \approx \pi$), one limb is moving down while the other is moving up. Relative phases between limbs are calculated every time a certain target limb passes through the absolute phase 0.

An experiment consists of a series of trials starting in various initial relative phase patterns. The subject is instructed to maintain the prescribed initial pattern and to cycle her limbs smoothly and continuously at a frequency set by an auditory metronome. Although instructions emphasize maintaining a one-to-one relation between the limbs and the metronome, no particular phase relationship between the metronome and the limbs is specified. The metronome frequency is systematically increased during each trial. The subject is instructed that should she feel the pattern begin to change, she should not try to resist the change, but instead perform whatever pattern seems most comfortable. (Although not done so here, subjects are capable of switching to a previously specified pattern, if so instructed; Jeka and Kelso, 1989.) All subjects were able to perform the

initial patterns after one or two practice trials. Two types of trials were conducted: two-limb trials and four-limb trials. The results below are consistent across all subjects.

2.2. *Two-limb trials.* The limb pair cycled during two-limb trials can be classified as either *homologous*, the two arms or the two legs, or *nonhomologous*, one arm and one leg. Nonhomologous limbs can be either *ipsilateral*, on the same side of the body, or *contralateral*, on different sides of the body. The initial relative phase patterns for two-limb trials are in-phase and anti-phase.

When subjects cycled two homologous limbs they most often maintained either the in-phase or anti-phase pattern throughout the trial as the metronome frequency increased. However, when subjects cycled two nonhomologous limbs and started in the anti-phase pattern, they almost always switched to the in-phase pattern. Figure 1 shows a typical trial with two nonhomologous limbs starting in the anti-phase pattern. The relative phase between the arm and the leg is plotted as a function of time. Metronome frequencies are indicated below the time axis. As the metronome frequency increases, the subject switches from the anti-phase pattern to the in-phase pattern and then to a phase drifting behavior. Ipsilateral limb pairs switched from the anti-phase pattern at a lower average metronome frequency than contralateral limb pairs. Switches from the in-phase pattern to the anti-phase pattern were rarely seen. At high metronome frequencies in trials with nonhomologous limbs, phase locking was usually lost and the relative phase began to wrap through a series of values. This phase drifting was generally due to the legs cycling slower than the arms.

2.3. *Four-limb trials.* Eight different initial relative phase patterns were used in the four-limb trials. Four of these have analogies in quadruped

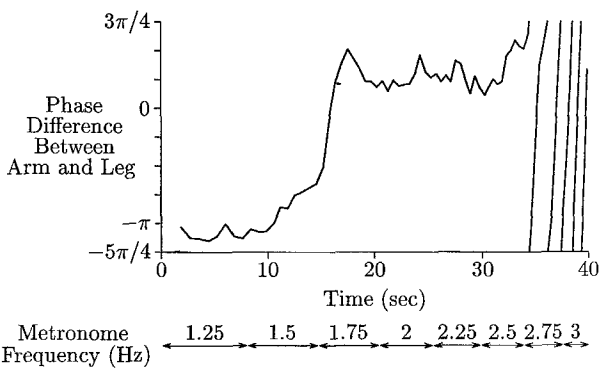

Figure 1. The relative phase between the right arm and the left leg in a two-limb trial showing a switch from the anti-phase ($\phi \approx \pi$) to the in-phase ($\phi \approx 0$) pattern.

locomotion, although their interpretation here in the context of human non-weight-bearing limb coordination is necessarily different. These are the *jump* (or *pronk*), in which all four limbs are in-phase, the *bound*, in which homologous limbs are in-phase and the non-homologous limbs are anti-phase, the *pace*, in which homologous limbs are anti-phase and ipsilateral limbs are in-phase, and the *trot*, in which homologous limbs are anti-phase and ipsilateral limbs are anti-phase. In the four other initial patterns, referred to as *tripod patterns*, three limbs are in-phase with each other and are anti-phase with the fourth limb. The tripod patterns will be designated with the anti-phase limb (e.g. right arm tripod).

Figure 2 shows a histogram of switches between patterns observed in three subjects. A switch from a pattern to itself indicates that the subject was able to maintain the pattern during the entire trial as the metronome frequency increased. The jump is the only pattern that was always maintained throughout the trial. In the other extreme the trot and the bound were never maintained throughout the trial; the trot always switched to the pace and the bound always switched to the jump. Tripod patterns showed a variety of switching behaviors. All four tripod patterns displayed transitions to the jump and pace, or between homologous and limb tripod patterns. For example, the left leg tripod switched to the jump, pace and right leg tripod, while the right arm tripod switched to the jump, pace or left arm tripod. In some cases the tripod patterns were maintained throughout the entire trial.

3. The model. In this section we describe a simple model of four coupled oscillators, which aims to capture some of the more robust dynamical behavior observed in the four-limb trials. We will use the results of the two-limb trials as motivation. The general form of the model, oscillators with additive relative-phase coupling, has often been used to model coupled oscillators (cf. Neu, 1979; Rand and Holmes, 1980; Cohen *et al.*, 1982; Haken *et al.*, 1985). The specifics of the model are an adaptation of the model of quadruped gaits presented in Schöner *et al.* (1990).

The model we consider treats each limb as an intrinsic oscillator with a stable limit cycle. Physiological studies indicate that the muscles and joints of an oscillating limb are constrained in such a way that the limb acts like a limit cycle oscillator; the limb undergoes a stable oscillation and returns to the oscillation after a perturbation (Orlovskii and Shik, 1965; Shik and Orlovskii, 1965; Pearson, 1976; Graham, 1985). The limit cycle a limb exhibits depends on the parameters of the system. In our experiments, the limbs are allowed to move about only one joint (the elbow or the knee) and only in the vertical plane.

The state of each oscillator in the model is given by its absolute phase, where the absolute phase of an uncoupled oscillator progresses linearly with time and advances by 2π during every cycle of oscillation. Since any two phases that

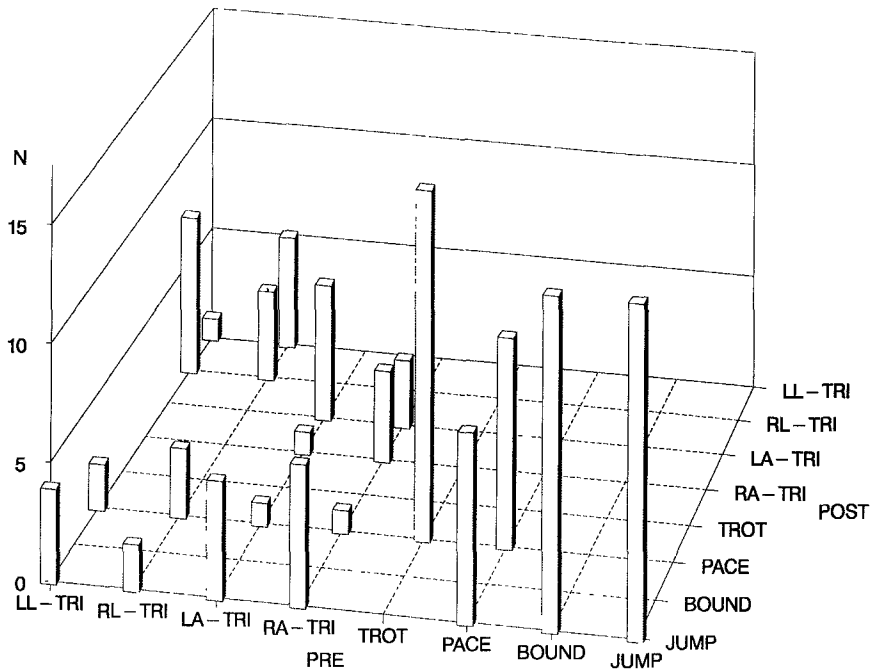

Figure 2. A histogram of pattern switching in four-limb trials. The PRE axis refers to patterns maintained before a transition (i.e. pre-transition) and the POST axis refers to patterns observed after a transition (i.e. post-transition). The total number of switches observed in three subjects from a pattern on the PRE axis to a pattern on the POST axis is plotted. A switch from a pattern to itself indicates that the pattern was maintained during the entire trial.

differ by a multiple of 2π can be considered identical, the state space for a single oscillator is a circle. In our case of four oscillators, we let $\theta_1, \theta_2, \theta_3$ and θ_4 be the absolute phases of the right arm, left arm, right leg and left leg, respectively. Phase $\theta_i = 0$ is defined to occur at the peak of each limb's upward position. We choose a model of the form:

$$\dot{\theta}_i = \omega_i + \sum_{j=1}^{4} f_{ij}(\theta_j - \theta_i), \cdot \text{ for } i = 1, \ldots, 4; \tag{1}$$

where the $\dot{\theta}_i$ indicates derivatives with respect to time and $f_{ii} \equiv 0$. The ω_i are the uncoupled angular frequencies of the limbs and the f_{ij} are 2π-periodic functions describing coupling from the jth to the ith oscillator. Since each θ_i lies on a circle, the state space of system (1) is the product of four circles, a four-dimensional torus.

Note that the metronome is not included in system (1). We view the metronome frequency as a parameter in the system which effects ω_i and f_{ij}. We do not include the absolute phase of the metronome in the model, because

subjects are not instructed to maintain any particular phase relationship with the metronome. In practice, the relative phases between the metronome and the limbs are not always the same for a given pattern and do not behave systematically during transitions between patterns.

System (1) assumes that the coupling between oscillators only depends on their relative phases and that coupling from multiple oscillators superimpose additively. This assumption of additive relative-phase coupling is motivated by general principles of coupled oscillators, rather than by the details of the multilimb system. Additive relative-phase coupling is a good *quantitative* approximation for weakly coupled oscillators whose intrinsic frequencies are close (Cohen *et al.*, 1982; Ermentrout and Kopell, 1984), or for strongly coupled oscillators whose interactions are appropriately dispersed throughout the cycle (Ermentrout and Kopell, 1991). Even for systems of oscillators not included in these cases, one expects that additive relative-phase coupling will often be a useful *qualitative* description. This is particularly plausible for the multilimb system, because the coupling between limbs is not especially strong; it typically takes several cycles to converge onto a pattern. Also, the behavior of two limbs is consistent with relative phases dynamics. For example, up and down oscillations in the relative phase are not observed.

We now consider the form of the functions f_{ij} in (1). Isolating two of the four limbs gives:

$$\begin{aligned} \dot{\theta}_i &= \omega_i + f_{ij}(\theta_j - \theta_i), \\ \dot{\theta}_j &= \omega_j + f_{ji}(\theta_i - \theta_j). \end{aligned} \tag{2}$$

Letting $\phi = \theta_i - \theta_j$ and $\Omega = \omega_i - \omega_j$, system (2) reduces to:

$$\dot{\phi} = \Omega + f_{ij}(-\phi) - f_{ji}(\phi). \tag{3}$$

Zeroes of the right hand side of equation (3) with a negative derivative correspond to stable relative phases between the two limbs. Recall that in two-limb trials relative phases between limbs near 0 (in-phase) or near π (anti-phase) are typically found. This suggests that equation (3) should take the qualitative form of:

$$\dot{\phi} = \Omega - a \sin(\phi) - b \sin(2\phi). \tag{4}$$

Equation (4) can be obtained from (3) by taking:

$$f_{ij}(\phi) = a_{ij} \sin(\phi) + b_{ij} \sin(2\phi), \tag{5}$$

for $i, j = 1, \ldots, 4$ with $i \neq j$, and letting $a = a_{ij} + a_{ji}$ and $b = b_{ij} + b_{ji}$. We will take equation (5) as our choice of the f_{ij}, although other choices are certainly possible. For example, an even function could be added to all the f_{ij}. This

addition would not change the relative phase equation (4), but would change the resulting frequency of the coupled oscillators. See Kopell (1988) for further discussion of this point.

Equation (4) has been derived from specific models of weakly coupled oscillators (Rand and Holmes, 1980; Haken *et al.*, 1985). With $\Omega=0$, it has been used as a model for two-hand coordination (Haken *et al.*, 1985) and with $\Omega\neq 0$, as a model for hand synchronization with a metronome (Kelso *et al.*, 1990).

Saddle-node bifurcations of (4), at which a stable fixed point and an unstable fixed point coalesce and disappear, are found by setting the right-hand side of (4) and its derivative equal to zero. This procedure yields:

$$\Omega=\sigma_2\left(\frac{3a+\sigma_1\sqrt{a^2+32b^2}}{4}\right)\sqrt{\frac{-a^2+16b^2+\sigma_1 a\sqrt{a^2+32b^2}}{32b^2}},$$

$$\phi=\sigma_2\cos^{-1}\left(\frac{-a+\sigma_1\sqrt{a^2+32b^2}}{8b}\right); \tag{6}$$

where $\sigma_1, \sigma_2=\pm 1$ (cf. Rand and Holmes, 1980). Figure 3 plots the bifurcation curves (6) in $(a/b, \Omega/b)$ parameter space for $b>0$. Regions of in-phase, anti-phase and drifting solutions are indicated. We use the terms in-phase and anti-phase loosely to indicate solutions with ϕ near 0 (between $-\pi/4$ and $\pi/4$) or near π (between $3\pi/4$ and $5\pi/4$), respectively. A drifting solution is a repetitive wrapping of ϕ around the circle, either in the upward or downward direction.

Having chosen the form of the f_{ij}, we now further constrain the behavior of system (1) by imposing left–right symmetry. Specifically, we assume that $\omega_1=\omega_2$, $\omega_3=\omega_4$, $f_{12}=f_{21}$, $f_{34}=f_{43}$, $f_{13}=f_{24}$, $f_{31}=f_{42}$, $f_{14}=f_{23}$ and $f_{41}=f_{32}$.

Since the coupling in system (1) only depends on relative phases, we can reduce the state space from a four-dimensional torus to a three-dimensional torus by using relative phase coordinates rather than absolute phase coordinates. Of the numerous relative phases one could consider, we chose the following since they behave nicely under left–right symmetry:

$$\begin{aligned}\phi_f&=\theta_1-\theta_2,\\ \phi_h&=\theta_3-\theta_4,\\ \phi_{fh}&=(\theta_1-\theta_3)+(\theta_2-\theta_4)=(\theta_1-\theta_4)+(\theta_2-\theta_3).\end{aligned} \tag{7}$$

Here ϕ_f is the phase between the arms (front limbs), ϕ_h is the phase between the legs (hind limbs) and ϕ_{fh} is the sum of the phase between the two right limbs

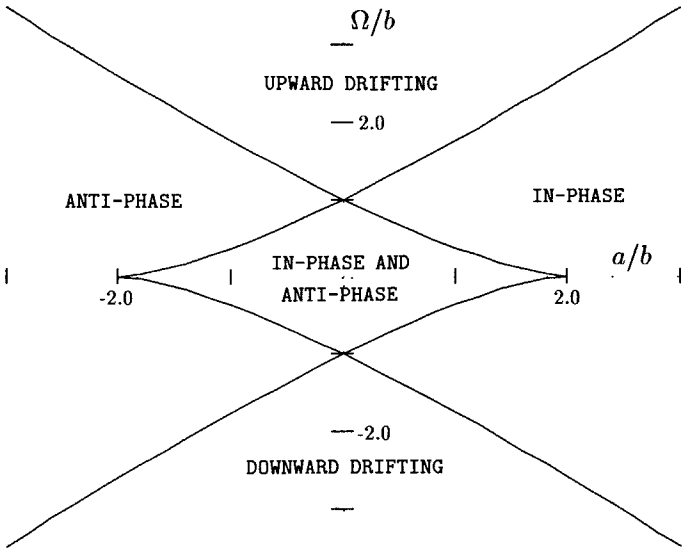

Figure 3. Bifurcation diagram for the flow (4) on a circle.

and the phase between the two left limbs. The relative phases, $\phi_{ij}=\theta_i-\theta_j$, between limbs are given in terms of the coordinate system (7) by:

$$\phi_{12}=\phi_f,\ \phi_{13}=\frac{1}{2}(\phi_{fh}+\phi_f-\phi_h),\ \phi_{14}=\frac{1}{2}(\phi_{fh}+\phi_f+\phi_h),$$

$$\phi_{34}=\phi_h,\ \phi_{24}=\frac{1}{2}(\phi_{fh}-\phi_f+\phi_h),\ \phi_{23}=\frac{1}{2}(\phi_{fh}-\phi_f-\phi_h). \tag{8}$$

The ϕ_{ij} as functions of ϕ_f, ϕ_h and ϕ_{fh} in equation (8) are invariant, modulo 2π, under the transformations:

$$(\phi_f+2\pi,\ \phi_h,\ \phi_{fh})\to(\phi_f,\ \phi_h,\ \phi_{fh}+2\pi),$$

$$(\phi_f,\ \phi_h+2\pi,\ \phi_{fh})\to(\phi_f,\ \phi_h,\ \phi_{fh}+2\pi),$$

$$(\phi_f,\ \phi_h,\ \phi_{fh}+4\pi)\to(\phi_f,\ \phi_h,\ \phi_{fh}). \tag{9}$$

Therefore, we use as our state space the box $\{\kappa_f\leqslant\phi_f\leqslant\kappa_f+2\pi,\ \kappa_h\leqslant\phi_h\leqslant\kappa_h+2\pi,\ \kappa_{fh}\leqslant\phi_{fh}\leqslant\kappa_{fh}+4\pi\}$ with the sides identified by (9) to form a three-dimensional torus. The constants κ_f, κ_h and κ_{fh} here are arbitrary. Table 1 gives the coordinates of the eight prototypical patterns. As mentioned above, a

Table 1. Coordinates of the eight prototypical patterns

Pattern	ϕ_f	ϕ_h	ϕ_{fh}
Jump	0	0	0
Bound	0	0	2π
Pace	π	π	0
Trot	π	π	2π
Right arm tripod	π	0	π
Left arm tripod	π	0	3π
Right leg tripod	0	π	3π
Left leg tripod	0	π	π

pattern that is close to one of the eight prototypical patterns will be referred to by the same name as its prototype.

Applying the change of coordinates (7) and imposing right–left symmetry system (1) becomes:

$$\begin{aligned}
\dot{\phi}_f &= f_{12}(-\phi_f) - f_{12}(\phi_f) \\
&\quad + f_{13}(-\phi_{fh}/2 - \phi_f/2 + \phi_h/2) - f_{13}(-\phi_{fh}/2 + \phi_f/2 - \phi_h/2) \\
&\quad + f_{14}(-\phi_{fh}/2 - \phi_f/2 - \phi_h/2) - f_{14}(-\phi_{fh}/2 + \phi_f/2 + \phi_h/2), \\
\dot{\phi}_h &= f_{34}(-\phi_h) - f_{34}(\phi_h) \\
&\quad + f_{31}(\phi_{fh}/2 + \phi_f/2 - \phi_h/2) - f_{31}(\phi_{fh}/2 - \phi_f/2 + \phi_h/2) \\
&\quad + f_{41}(\phi_{fh}/2 - \phi_f/2 - \phi_h/2) - f_{41}(\phi_{fh}/2 + \phi_f/2 + \phi_h/2), \\
\dot{\phi}_{fh} &= 2\delta + f_{12}(\phi_f) + f_{12}(-\phi_f) - f_{34}(\phi_h) - f_{34}(-\phi_h) \\
&\quad + f_{13}(-\phi_{fh}/2 - \phi_f/2 + \phi_h/2) + f_{13}(-\phi_{fh}/2 + \phi_f/2 - \phi_h/2) \\
&\quad - f_{31}(\phi_{fh}/2 + \phi_f/2 - \phi_h/2) - f_{31}(\phi_{fh}/2 - \phi_f 2 + \phi_h/2) \\
&\quad + f_{14}(-\phi_{fh}/2 - \phi_f/2 - \phi_h/2) + f_{14}(-\phi_{fh}/2 + \phi_f/2 + \phi_h/2) \\
&\quad - f_{41}(\phi_{fh}/2 - \phi_f/2 - \phi_h/2) - f_{41}(\phi_{fh}/2 + \phi_f/2 + \phi_h/2),
\end{aligned} \tag{10}$$

where $\delta = \omega_1 - \omega_3$. As desired, system (10) displays the left–right symmetry clearly as an invariance under the transformation $(\phi_f, \phi_h, \phi_{fh}) \to (-\phi_f, -\phi_h, \phi_{fh})$.

4. Invariant circles. We now consider subspaces that are invariant under the flow of system (10) and attract all nearby points in the state space. The dynamics on these attracting invariant subspaces reveal much of the dynamics of the full system.

4.1. *Bound-jump invariant circle.* If $\phi_f = \phi_h = 0$, then:

$$\begin{aligned}
\dot{\phi}_f &= \dot{\phi}_h = 0, \\
\dot{\phi}_{fh} &= 2\delta + 2f_{12}(0) - 2f_{34}(0) \\
&\quad + 2f_{13}(-\phi_{fh}/2) - 2f_{31}(\phi_{fh}/2) \\
&\quad + 2f_{14}(-\phi_{fh}/2) - 2f_{41}(\phi_{fh}/2), \\
&= 2\delta - 2(a_{13} + a_{31} + a_{14} + a_{41})\sin(\phi_{fh}/2) \\
&\quad - 2(b_{13} + b_{31} + b_{14} + b_{41})\sin(\phi_{fh}).
\end{aligned} \tag{11}$$

Therefore, the set $\phi_f = \phi_h = 0$ is invariant. This set, shown as a vertical line in Fig. 4, has the topology of a circle, since the top and bottom of the box in Fig. 4 are identified. To study when this invariant circle is attracting we calculate the linearization of $\dot{\phi}_f$ *and* $\dot{\phi}_h$ around the subspace:

$$\begin{pmatrix} \dot{\phi}_f \\ \dot{\phi}_h \end{pmatrix} = M \begin{pmatrix} \phi_f \\ \phi_h \end{pmatrix}; \tag{12}$$

where

$$M = \begin{pmatrix} -2f'_{12}(0) - f'_{13}\left(\frac{-\phi_{fh}}{2}\right) - f'_{14}\left(\frac{-\phi_{fh}}{2}\right) & f'_{13}\left(\frac{-\phi_{fh}}{2}\right) - f'_{14}\left(\frac{-\phi_{fh}}{2}\right) \\ f'_{31}\left(\frac{\phi_{fh}}{2}\right) - f'_{41}\left(\frac{\phi_{fh}}{2}\right) & -2f'_{34}(0) - f'_{31}\left(\frac{\phi_{fh}}{2}\right) - f'_{41}\left(\frac{\phi_{fh}}{2}\right) \end{pmatrix}.$$

If:

$$\begin{aligned}
f'_{12}(0) &> \max_{\phi} \{|f'_{13}(\phi)|, |f'_{14}(\phi)|\} \text{ and} \\
f'_{34}(0) &> \max_{\phi} \{|f'_{31}(\phi)|, |f'_{41}(\phi)|\},
\end{aligned} \tag{13}$$

then $M_{11} + |M_{12}| < -\rho$ and $M_{22} + |M_{21}| < -\rho$ for some $\rho > 0$. If $|\phi_f| \geq |\phi_h|$, then $\mathrm{d}|\phi_f|/\mathrm{d}t \leq M_{11}|\phi_f| + |M_{12}||\phi_h| \leq M_{11}|\phi_f| + |M_{12}||\phi_f| \leq -\rho|\phi_f|$. Similarly, if $|\phi_h| \geq |\phi_f|$, then $\mathrm{d}|\phi_h|/\mathrm{d}t \leq -\rho|\phi_h|$. Combining these two inequalities, we have:

$$\frac{\mathrm{d}}{\mathrm{d}t} \max\{|\phi_f|, |\phi_h|\} \leq -\rho \max\{|\phi_f|, |\phi_h|\};$$

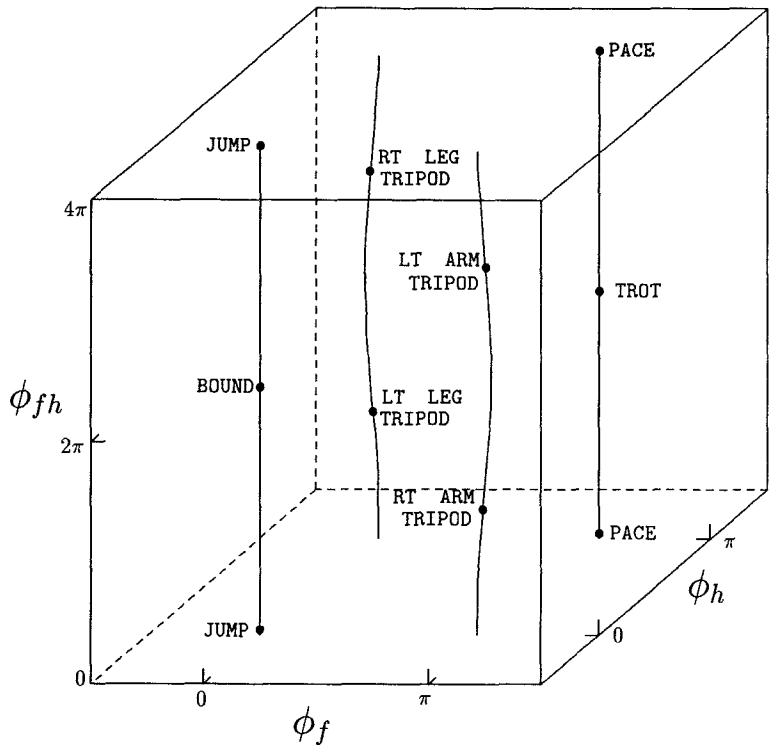

Figure 4. Invariant circles of the model. Four periodic trajectories with parameter values $a_{12}=a_{34}=a_{31}=a_{14}=a_{41}=0$, $a_{13}=0.15$, $b_{12}=b_{34}=1$, $b_{13}=b_{31}=b_{14}=b_{41}=0.3$ *and* $\Delta=1.5$ are shown. Here, the detuning parameter Δ was chosen sufficiently large to prevent phase locking.

implying that nearby trajectories approach the invariant circle exponentially fast. Therefore, inequalities (13) give sufficient conditions for the circle $\phi_f=\phi_h=0$ to be an attracting invariant subspace.

The result above states that if the in-phase coupling of the homologous limbs is stronger than coupling between nonhomologous limbs, then when both pairs of homologous limbs start in-phase, they will remain in-phase. In this case the dynamics are constrained to lie on a circle containing the bound and the jump (see Fig. 4). Note from (11) that the flow on this circle has the same form as the flow (4) describing the coordination between two limbs. Letting $a=a_{13}+a_{31}+a_{14}+a_{41}$, $b=b_{13}+b_{31}+b_{14}+b_{41}$ and $\Omega=\delta$, Fig. 3 can now be interpreted to give regions in parameter space in which the jump (in-phase), bound (anti-phase) or drifting through the two patterns occur.

4.2. *Trot–pace invariant circle.* Analogous to the invariant circle $\phi_f=\phi_h=0$ containing the bound and the jump, there is an invariant circle containing the trot and the pace. If $\phi_f=\phi_h=\pi$, then:

$$\begin{aligned}
\dot{\phi}_f &= \dot{\phi}_h = 0, \\
\dot{\phi}_{fh} &= 2\delta + 2f_{12}(\pi) - 2f_{34}(\pi) \\
&\quad + 2f_{13}(-\phi_{fh}/2) - 2f_{31}(\phi_{fh}/2) \\
&\quad + 2f_{14}(-\phi_{fh}/2 + \pi) - 2f_{41}(\phi_{fh}/2 + \pi) \\
&= 2\delta - 2(a_{13} + a_{31} - a_{14} - a_{41})\sin(\phi_{fh}/2) \\
&\quad - 2(b_{13} + b_{31} + b_{14} + b_{41})\sin(\phi_{fh}).
\end{aligned} \tag{14}$$

Sufficient conditions for the invariant circle $\phi_f = \phi_h = \pi$ to be attracting are:

$$\begin{aligned}
f'_{12}(\pi) &> \max_{\phi} \{|f'_{13}(\phi)|, |f'_{14}(\phi)|\} \text{ and} \\
f'_{34}(\pi) &> \max_{\phi} \{|f'_{31}(\phi)|, |f'_{41}(\phi)|\}.
\end{aligned} \tag{15}$$

Letting $a = a_{13} + a_{31} - a_{14} - a_{41}$, $b = b_{13} + b_{31} + b_{14} + b_{41}$ and $\Omega = \delta$, Fig. 3 now describes regions in parameter space in which the pace (in-phase), trot (anti-phase) or drifting through the two patterns occur. Figure 4 shows the trot–pace circle in state space.

4.3. *Tripod invariant circles.* Unlike the circles $\phi_f = \phi_h = 0$ and $\phi_f = \phi_f = \phi_h = \pi$, that are invariant under the flow of system (10) for all parameter values, there are invariant circles that only exist in certain parameter regimes. In this subsection we consider an invariant circle containing the right leg tripod and the left leg tripod patterns that exist if the coupling between homologous limbs is significantly stronger than the coupling between nonhomologous limbs. We express this difference in coupling strengths by letting $f_{ij} = \varepsilon F_{ij}$, $a_{ij} = \varepsilon A_{ij}$ and $b_{ij} = \varepsilon B_{ij}$ for $ij \in \{13, 31, 14, 41\}$, where $0 < \varepsilon \ll 1$. The coupling functions f_{12} and f_{34} remain of the order 1.

If the arms are stably in-phase ($\phi_f = 0$, $f'_{12}(0) > 0$), the legs are stably anti-phase ($\phi_f = \pi$, $f'_{34}(\pi) > 0$) and all connections between the arms and the legs are severed ($\varepsilon = 0$), then system (10) reduces to:

$$\begin{aligned}
\dot{\phi}_f &= \dot{\phi}_h = 0, \\
\dot{\phi}_{fh} &= 2\delta + 2f_{12}(0) - 2f_{34}(\pi) = 2\delta.
\end{aligned} \tag{16}$$

In this limiting case the circle $\{\phi_f = 0, \phi_h = \pi\}$ containing both leg tripods is invariant and attracting. This attracting invariant circle will persist if ε is sufficiently small, although in general its shape will become deformed (Hirsch *et al.*, 1977).

We now consider the flow on the invariant circle. Using $\phi_f = O(\varepsilon)$ and $\phi_h = \pi + O(\varepsilon)$, the expression for $\dot{\phi}_{fh}$ in (10) becomes:

$$\dot{\phi}_{fh} = 2\delta + 2f_{12}(0) - 2f_{34}(\phi)$$
$$+ \varepsilon F_{13}\left(-\frac{1}{2}\phi_{fh} + \frac{\pi}{2}\right) + \varepsilon F_{13}\left(-\frac{1}{2}\phi_{fh} - \frac{\pi}{2}\right)$$
$$- \varepsilon F_{31}\left(\frac{1}{2}\phi_{fh} - \frac{\pi}{2}\right) - \varepsilon F_{31}\left(\frac{1}{2}\phi_{fh} + \frac{\pi}{2}\right)$$
$$+ \varepsilon F_{14}\left(-\frac{1}{2}\phi_{fh} - \frac{\pi}{2}\right) + \varepsilon F_{14}\left(-\frac{1}{2}\phi_{fh} + \frac{\pi}{2}\right)$$
$$- \varepsilon F_{41}\left(\frac{1}{2}\phi_{fh} - \frac{\pi}{2}\right) - \varepsilon F_{41}\left(\frac{1}{2}\phi_{fh} + \frac{\pi}{2}\right) + O(\varepsilon^2).$$
$$= 2\delta + 2\varepsilon(B_{13} + B_{31} + B_{14} + B_{41})\sin(\phi_{fh}) + O(\varepsilon^2). \tag{17}$$

We note from (17) that phase locking is only possible if $\delta = O(\varepsilon)$. Therefore, we let $\delta = \varepsilon\Delta$ and write the flow on the invariant circle as:

$$\dot{\phi}_{fh} = \varepsilon[2\Delta + 2(B_{13} + B_{31} + B_{14} + B_{41})\sin(\phi_{fh})] + O(\varepsilon^2). \tag{18}$$

The bifurcation diagram for (18) is given by Fig. 3, with $a = 0$, $b = B_{13} + B_{31} + B_{14} + B_{41} + O(\varepsilon)$ and $\Omega = \Delta$. Arbitrarily, we let in-phase refer to the right leg tripod pattern and anti-phase to the left leg tripod pattern. When $\Delta = 0$ the flow (18) has stable fix points at $\phi_{fh} = \pi + O(\varepsilon)$ and $\phi_{fh} = 3\pi + O(\varepsilon)$, corresponding to the left leg tripod and the right leg tripod, respectively (see Table 1). As Δ passes upwards through $B_{13} + B_{31} + B_{14} + B_{41} + O(\varepsilon)$, both tripod patterns cease to be fixed points simultaneously and upward drifting begins.

Analogous to the leg tripod circle described above, there is an invariant circle containing the arm tripod patterns (see Fig. 4). The flow on the arm tripod circle has the same form as (18).

5. Discussion. In this section we compare the behavior of the model to the behavior of the experimental system. Specifically, we examine whether the invariant circles of the model are reflected in the dynamics of the limb movements of the subjects and, if so, whether the direction of switches between two patterns on the same circle can be interpreted by the model.

We saw above that the model has four attracting invariant circles (bound–jump, trot–pace, arm tripod and leg tripod), if the coupling between homologous limbs is sufficiently stronger than the coupling between non-homologous limbs. Even though Fig. 2 shows that switches are observed between invariant circles (e.g. right arm tripod to jump), the majority of

transitions are observed within a circle. In particular, there are no switches out of the bound–jump circle, all switches from the trot go to the pace and a number of switches occur between tripod patterns on the same circle.

Figure 5 shows trajectories in state space of one subject. Five trials starting in each of the eight patterns are plotted. There is a strong indication of the bound–jump circle and the leg tripod circle, as well as some evidence of the trot–pace circle (cf. Fig. 4). Although there are trajectories between circles, most trajectories between patterns lie near the circles of the model. The circles most evident vary with subject. Only the bound–jump circle was clearly seen in all three subjects.

We now restrict our attention to switches between patterns on the same circle. Recall from Fig. 2 that there are switches in both directions on the two tripod circles, but switches only occur from bound to jump on the bound–jump circle and only from trot to pace on the trot–pace circle. Our goal is to interpret these results based on our knowledge of two-limb coordination.

If we consider coordination between the two limbs i and j with $i<j$, then

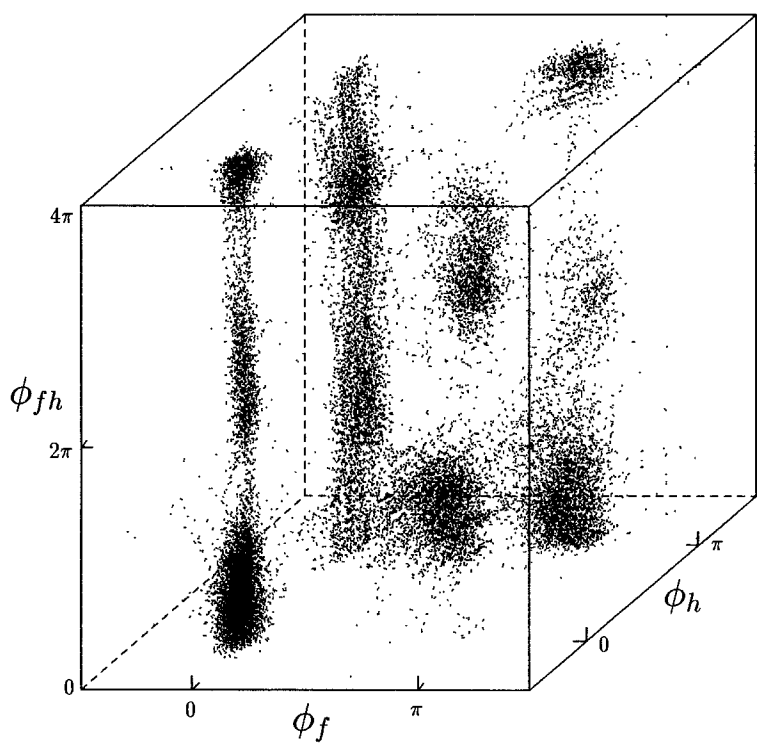

Figure 5. Phase trajectories of the subject GP from all the experimental four-limb trials. Dotted lines connect measured three-dimensional points of the relative phase used to characterize the four-limb patterns. Note that trajectories accumulate close to the invariant circles from the model.

Fig. 3 is the bifurcation diagram for their dynamics, where $a=a_{ij}+a_{ji}$, $b=b_{ij}+b_{ji}>0$ and $\Omega=\omega_i-\omega_j$. During a trial we imagine the point $(a/b, \Omega/b)$ in parameter space varying as the metronome frequency is increased. The experimental two-limb data suggest the following dependence of the parameters on metronome frequency. For two homologous limbs $\Omega=0$ and $(a/b, \Omega/b)$ remains within the region of Fig. 3, in which both the in-phase and anti-phase patterns are stable. For two nonhomologous limbs $\Omega=\omega_1-\omega_3$ and $(a/b, \Omega/b)$ moves from the region of bistability, through the region in which only the in-phase pattern is stable and into the region of upward drifting. Based on this description we assume that $a>0$ and $\omega_1-\omega_3$ is an increasing function of metronome frequency. Although not strictly necessary for the discussion that follows, for simplicity we also assume that a and b do not vary with metronome frequency. Not that under these assumptions, the size of a determines the frequency at which the anti-phase pattern is lost. If a is increased the anti-phase pattern is lost at a lower metronome frequency.

The bifurcation diagram for the dynamics on the bound–jump circle is given by Fig. 3 with $a=a_{13}+a_{31}+a_{14}+a_{41}$, $b=b_{13}+b_{31}+b_{14}+b_{41}$ and $\Omega=\omega_1-\omega_3$. Here, in-phase refers to the jump and anti-phase refers to the bound. Since we are assuming that $a_{13}+a_{31}>0$ and $a_{14}+a_{41}>0$ based on two-limb dynamics, we have $a>0$. Therefore, as Ω increases with metronome frequency the model suggests that the bound should switch to the jump. This is the direction of switches found in the four-limb trials.

The bifurcation diagram for the dynamics on a tripod circle is given by Fig. 3, with $a=0$, $b_{13}+b_{31}+b_{14}+b_{41}=\varepsilon b+O(\varepsilon^2)$ and $\omega_1-\omega_3=\varepsilon\Omega$, where $\varepsilon\ll 1$ is the ratio between nonhomologous coupling strength and homologous coupling strength. In-phase and anti-phase refer arbitrarily to the two tripod patterns on the circle. Since parameters are constrained to the vertical axis of Fig. 3, both tripod patterns cease to be fixed points simultaneously as Ω increases. Instead the solution continuously wraps around the circle with ϕ_{fh} increasing, slowing each time it passes through one of the two tripod patterns. This description is consistent with the experimental results, except that fluctuations not in the model appear to cause premature switches between tripod patterns on the same circle. Elsewhere, fluctuations have been explicitly taken into account in theoretical and empirical studies of interlimb coordination (Schöner *et al.*, 1986; Kelso *et al.*, 1986), but we do not pursue this further here.

Finally, the bifurcation diagram for the dynamics on the trot–pace circle is given by Fig. 3, with $a=a_{13}+a_{13}+a_{14}-a_{41}$, $b=b_{13}+b_{31}+b_{14}+b_{41}$ and $\Omega=\omega_1-\omega_3$. In-phase refers to the pace and anti-phase refers to the trot. As with the bound–jump circle, we assume that $a_{13}+a_{31}>0$ and $a_{14}+a_{41}>0$. However, now these inequalities do not determine the sign of a. Recalling from the two-limb trials that ipsilateral nonhomologous limbs lose the anti-phase

pattern at a lower average metronome frequency than contralateral nonhomologous limbs, we assume that $a_{13}+a_{31}<a_{14}+a_{41}$. Therefore, $a>0$, which in turn implies that the trot should switch to the pace as the metronome frequency increases. This direction of pattern switching matches the experimental four-limb data.

In summary, much of the behavior of the experimental multilimb system can be interpreted by the model. The experimental trajectories of the relative phase usually lie near the invariant circles of the model (compare Fig. 4 and 5) and the direction of switches between two patterns on the same circle is consistent with data from two-limb trials.

There is much general interest now in phase and frequency synchronization in neurobiological systems. Such phenomena have been observed in many systems and at different levels. The present approach interprets switches in the pattern of coordination between limbs as bifurcations in a dynamical system. Some of the mathematical concepts employed (symmetry, invariant subspaces, etc.) may be generally useful in the analysis of other systems. At the same time our approach affords further experimental explorations, for example, of transition pathways and preferred routes among multiple patterns in the present experimental model system.

This research was supported by an NIMH (Neurosciences Research Branch) grant MH42900-01 and contract N00014-88-J-119 from the U.S. Office of Naval Research. T.K. was supported by NIMH training grant MH19116-01 at FAU and an NSF postdoctoral fellowship at NIH. We thank Jose Gonzalez-Fernandez and John Rinzel for reading the manuscript.

LITERATURE

Cohen, A. H., P. J. Holmes and R. H. Rand. 1982. The nature of the coupling between segmental oscillators of the lamprey spinal generator for locomotion: A mathematical model. *J. math. Biol.* **13**, 345–369.

Ermentrout, G. B. and N. Kopell. 1984. Frequency plateaus in a chain of weakly coupled oscillators, I. *SIAM J. math. Anal.* **15** (2), 215–237.

Ermentrout, G. B. and N. Kopell. 1991. Multiple pulse interactions and averaging in systems of coupled neural oscillators. *J. math. Biol.* **29**, 195–217.

Graham, D. 1985. Pattern and control of walking in insects. *Adv. Insect Physiol.* **18**, 31–40.

Haken, H., J. A. S. Kelso and H. Bunz. 1985. A theoretical model of phase transitions in human hand movements. *Biol. Cybern.* **51**, 347–356.

Hirsch, M. W., C. C. Pugh and M. Shub. 1977. *Invariant Manifolds*. New York: Springer-Verlag.

Jeka, J. J. and J. A. S. Kelso. 1989. Pattern formation in a multistable coordinative system. *Soc. Neurosci. Abstr.* **15** (1), 605.

Kelso, J. A. S. 1984. Phase transitions and critical behavior in human bimanual coordination. *Am. J. Physiol. Regul. Intergr. comp. Physiol.* **15**, R1000–R1004.

Kelso, J. A. S. and J. J. Jeka. 1992. Symmetry breaking dynamics of human multilimb coordination. *J. exp. Psychol. Hum. Percept. Perf.*, **18**(3), 645–668.

Kelso, J. A. S., J. D. Delcolle and G. S. Schöner. 1990. Action-perception as a pattern formation

process. In *Attention and Performance XIII*. M. Jeannerod (Ed.), pp. 139–169. Hillsdale, NJ: Erlbaum.

Kelso, J. A. S., J. P. Scholz and G. S. Schöner. 1986. Non-equilibrium phase transitions in coordinated biological motion: Critical fluctuations. *Phys. Lett.* **A118**, 279–284.

Kopell, N. 1988. Toward a theory of modelling central pattern generators. In *Neural Control of Rhythmic Movements in Vertebrates*. A. H. Cohen, S. Rossignol and S. Grillner (Eds), pp. 369–413. New York: John Wiley.

Neu, J. C. 1979. Coupled chemical oscillators. *SIAM J. appl. Math.* **37** (2), 307–315.

Orlovskii, G. N. and M. L. Shik. 1965. Standard elements of cyclic movement. *Biophys.* **10,** 935–944.

Pearson, K. G. 1976. The control of walking. *Sci. Am.* **235** (6), 72–86.

Rand, R. H. and P. J. Holmes. 1980. Bifurcation of periodic motions in two weakly coupled van der Pol oscillators. *Int. J. non-linear Mech.* **15**, 387–399.

Schöner, G. S., H. Haken and J. A. S. Kelso. 1986. A stochastic theory of phase transitions in human hand movement. *Biol. Cybern.* **53**, 442–452.

Schöner, G., W. Y. Jiang and J. A. S. Kelso. 1990. A synergetic theory of quadrupedal gaits and gait transitions. *J. theor. biol.* **142** (3), 359–393.

Shik, M. L. and G. N. Orlovskii. 1965. Co-ordination of the limbs during running of the dog. *Biophys.* **10**, 1148–1159.

Received 18 November 1991
Revised 22 June 1992